Impact of organic templates on the selective formation of zeolite oligomers

Marine Ciantar,[a] Thuat T. Trinh,[b] Carine Michel,[b] Philippe Sautet,[b,c,d] Caroline Mellot-Draznieks,*[e] Carlos Nieto-Draghi*[a]

[a] Dr. M. Ciantar, Dr. Carlos Nieto-Draghi
IFP Energies nouvelles, 1-4 Avenue de Bois-Préau, 92852 Rueil-Malmaison, France
E-mail: carlos.nieto@ifpen.fr
[b] Dr. T. T. Trinh, Dr. C. Michel, Prof. P. Sautet
Univ Lyon, Ens de Lyon, CNRS UMR 5182, Université Claude Bernard Lyon 1, Laboratoire de Chimie, F69342, Lyon, France
[c] Department of Chemical and Biomolecular Engineering, University of California, Los Angeles, Los Angeles, California 90095, United States
[d] Department of Chemistry and Biochemistry, University of California, Los Angeles, Los Angeles, California 90095, United States
[e] Dr. Caroline Mellot-Draznieks.
Laboratoire de Chimie des Processus Biologiques. UMR CNRS 8229, Collège de France, Sorbonne Université,
PSL Research University. 11 Place Marcelin Berthelot, 75231 Paris, Cedex 05, France
E-mail: caroline.mellot-draznieks@college-de-france.fr

Supporting information for this article is given via a link at the end of the document.

Abstract: Zeolites are essential materials to industry due to their adsorption and catalytic properties. The best current approach to prepare a targeted zeolite still relies on trial and error's synthetic procedures since a rational understanding of the impact of synthesis variables on the final structures is still missing. To discern the role of a variety of organic templates, we perform simulations of the early stages of condensation of silica oligomers by combining DFT, Brønsted-Evans-Polanyi relationships and kinetic Monte Carlo simulations. We investigate an extended reaction path mechanism including 258 equilibrium reactions and 242 chemical species up to silica octamers, comparing the computed concentrations of Si oligomers with ^{29}SI NMR experimental data. The effect of the templating agent is linked to the modification of the intramolecular H-bond network in the growing oligomer, which produces higher concentration of 4-membered ring intermediates, precursors of the key double-four ring building blocks present on more than 39 known zeolite topologies.

Introduction

Zeolites are porous crystalline materials currently used in the petrochemical industry for their outstanding absorption properties and their catalytic activities (separation and capture, refining...). The latter are recognized as highly dependent on the atomic-level structure of zeolites, in terms of pores' shape and channels' connectivity, amongst others. The understanding of the very early stages of oligomerisation in solution which are known to play a decisive role in determining the final structure of zeolites is thus required to achieve a control of their properties [1]. The nucleation rate depends on many parameters (for example Si/Al ratio, aging, stirring, pH, initial concentrations, temperature...) that determine the resulting zeolitic structure. In particular, the nature of the templating (organic or inorganic) agent in the solution is known to play a crucial role in the nucleation process [2]. The experimental characterisation of the first steps of oligomerisation and nucleation of zeolites is extremely challenging as a result of the complexity of the reaction process and small nuclei sizes involved, combined with the very short lifetime of the reactive species. Precursors have been mainly followed by NMR [3,4], mass spectroscopy and in situ X-ray scattering techniques [5,6]. By contrast, many simulation studies have explored the reaction pathways in solution [7,8,9,10,11,12,13], shedding light on the nature and structure of initial silicate oligomers, ranging from small oligomers to larger cyclic species [10,11,14]. These computational studies exploring the oligomerisation process of silicates have included the impact of small cationic templates (Li^+, NH_4^+) [15]. However, very scarce atomistic simulation works were devoted to elucidate the specific influence of commonly used templates (tetramethylamine-TMA^+, tetraethylamine-TEA^+ and tetrapropylamine-TPA^+ ions) in the silica condensation process [12, 16, 17]. In order to move to higher time and space scales, kinetic Monte Carlo (kMC) methods are particularly appropriate, where rate constants obtained from quantum calculations are used as the main input. They can thus follow the time evolution of a complex reaction network, that cannot be easily inferred from the direct examination of activation barriers and the relative thermodynamic stability of intermediate species [18,19,20]. Also, kMC methods allow investigating the effect of relevant macroscopic parameters such as pH, temperature [21,22,23] and counterions such as Li^+ and NH_4^+ [15, 24, 25, 26] on the oligomerisation kinetics.

In the present work, we investigate and discuss the structure-directing role of a variety of organic molecules such as TPA^+, TEA^+ and TMA^+ using a multiscale computational approach. Focusing on synthesis operated at a basic pH, we propose an anionic reaction mechanism and compute at the density functional theory (DFT) level the corresponding barriers for the formation of oligomers (dimer, linear trimer to hexamer, cyclic trimers to hexamer, branched tetramer and pentamer, see Figure S2 and Table S1) in the presence or the absence of a template. In order to expand the reaction network up to octamers, the activation barriers for larger oligomers were derived in a second step using Brønsted-Evans-Polanyi (BEP) relationships. Finally, both the DFT- and BEP-derived energies were then used in kMC calculations to estimate the concentration profiles of all oligomers in solution with and without template.

Results and Discussion

The oligomeric condensation in basic conditions obeys an anionic mechanism whereby the Si-O$^-$ group of the growing oligomer $\mathbf{R_i}$ reacts with an $Si(OH)_4$ monomer, following an addition/elimination sequence shown in Scheme 1 involving a five-coordinated intermediate, $\mathbf{I_i}$. The formed water molecule is H-bonded to the oligomer in the hydrated product $\mathbf{P_i}$. It is subsequently eliminated, substituted by a $Si(OH)_4$ monomer to give $\mathbf{R_{i+1}}$ and initiate the next growth step. An analogous cyclisation mechanism was also considered, whereby the $Si(OH)_4$ monomer is replaced by a -SiOH group of the cyclizing oligomer.

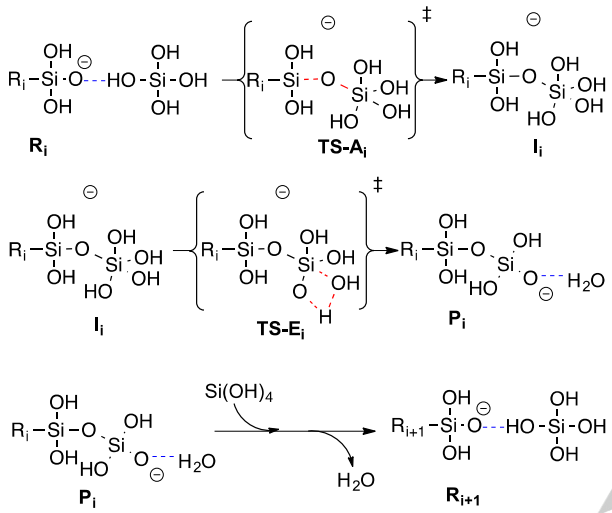

Scheme 1. Anionic concerted mechanism in basic conditions proposed for the formation of linear oligomers. The reactive complex ($\mathbf{R_i}$) formed of the anionic oligomer and an $Si(OH)_4$ monomer undergoes an addition reaction ($\mathbf{TS\text{-}A_i}$) yielding a five-coordinated intermediate ($\mathbf{I_i}$). The elimination of water ($\mathbf{TS\text{-}E_i}$) allows the formation of a hydrated complex ($\mathbf{P_i}$). The exchange of the water molecule with a monomer results in the reactant complex $\mathbf{R_{i+1}}$. (see also the mechanisms for cyclic and branched oligomers in **Schemes S1** and **S2,** respectively). **TS** stands for transition state.

We investigated the early stages of oligomerisation, starting from $\mathbf{R_0}$ ($Si(OH)_3O^-$) up to linear, branched and cyclic hexameric oligomers $\mathbf{R_5}$. The relative Gibbs Free energies were computed at the B98D/311+g(d,p) level of theory, the aqueous solvent being taken into account using the Conductor-like Polarizable Continuum Model (CPCM) using Gaussian09 [27]. Those oligomers are highlighted with a yellow background in Scheme 2, where a selection of some typical intermediates from $\mathbf{R_0}$ to $\mathbf{R_7}$ are represented, the environment of each Si being colour-coded in terms of its Si-O-Si connectivity. This is typically expressed as Q^n following the notation used in ^{29}Si-NMR spectroscopy where n is the number of 'Si' units attached through a bridging oxygen to an individual SiO_4 unit: Q^0 for monomers, Q^1 for Si-O-Si dimers (in black), Q^2 for Si-O-Si-O-Si chains (in red), Q^3 (in orange) and Q^4 (in green) for branched oligomers. We used this connectivity descriptor for all oligomers in this study since this is the essential one monitored by ^{29}SI NMR experiments [28, 29].

As expected, the oligomerisation is found exergonic and larger species are more stable in solution than small ones, regardless of the oligomer topology (linear, branched or cyclic) and in agreement with previous reports [20,30,31,32]. However, the reaction profile depends on the oligomer topology and more importantly, the effect of the templating agents (TMA^+, TEA^+ and TPA^+) varies from one topology to the next, as summarized below (see SI for more details)

For linear species, increasing the chain's length requires to overcome barriers of around +50-60 kJ.mol^{-1}, and templates only have a marginal effect on the barrier. The branching of silica oligomers is less demanding regarding the activation barriers, which are below +52 kJ.mol^{-1}, making the branching more likely than the increase in the chain's length according to our DFT profiles. Furthermore, the effect of templates is more contrasted on the branching reactions than on the increase of the chain's length. During the formation of a branched tetramer from a linear trimer, all three templates systematically destabilize the whole Gibbs Free Energy by ~ +20 kJ.mol^{-1} (see Figure S1.a), which should strongly limit the branching process at that stage. Notably, TMA^+ and TEA^+ facilitate the water elimination for a branched pentamer (see Figure S2.h). Last, in the absence of template, the cyclisation is favoured for large cycles, with barriers below 50 kJ.mol^{-1} for the cyclic pentamer and hexamer. This situation is strongly modified in the presence of templates. While they only slightly affect the profile for the cyclic pentamer (see Figure S1.a and Scheme S1), the templates strongly hamper the cyclic hexamer formation (Figure S2.j).

Overall, the results above suggest that in templated synthesis of zeolites the ratio of linear/branched/cyclic oligomers may be tuned by the choice of the template thanks to its interactions with the pentacoordinated intermediate, $\mathbf{I_i}$, and the possibility of stabilising additional intramolecular H-bonds within the silica oligomer (see the Non-Covalent Interaction analysis (NCI)[33,34] provided in SI). The branched tetramer appears as hampered by the presence of a template while the formation of 5 membered rings is not affected. However, no firm conclusions can be automatically drawn from Gibbs Free energy profiles since the effect of relative concentrations and diffusion limitations are not included yet. For instance, despite the fact that the cyclisation of large cycles is a low barrier process, it will be limited by the concentration of the corresponding linear oligomer.

In a further step, we performed kMC simulations using our DFT energies to estimate steady state concentrations of species. One of the key assets of kMC simulations on oligomerisation reactions is the possibility to handle both diffusive and reactive events at the same time. The implementation of the "Reacdiff" module in the SPPARKS parallel kMC code reported in our previous work [31] allowed us to model every step of Scheme 1 on large systems sizes, including the last step, whereby the diffusion of fresh $Si(OH)_4$ monomer encounters the hydrated complex ($\mathbf{Pi}$) to release one water molecule to pursue the oligomerisation mechanism with the formation of $\mathbf{R_{i+1}}$. Another important advantage of kMC simulations is the ability to impose a pH for the initial conditions of the condensation process in a liquid phase through the initial concentrations of species [31]. In this previous work, we highlighted the impact of the pH, the initial concentration of SiOH and the diffusion coefficient. The most favourable conditions to grow oligomers appeared to be a pH of 9 and a hypersaturated concentration of 1 mol.L^{-1}, in agreement with experimental investigations. In this work, a pH of 9 was thus imposed by fixing the initial ratio of neutral/anionic

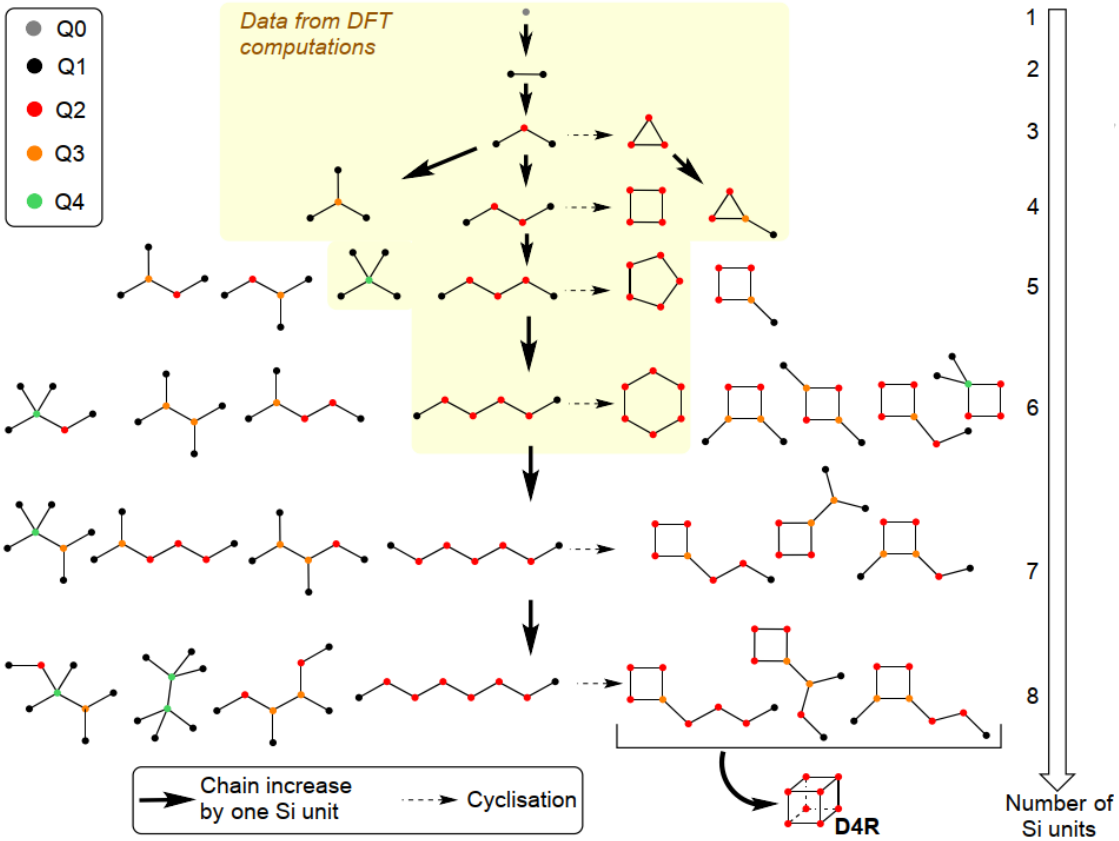

Scheme 2. Simplified representation of the oligomerisation network up to the octamers showing a selection of the 252 oligomers considered in this work, including some plausible precursors of a double-four ring D4R (this specific structure is not included in the kMC simulations). Oligomers are obtained by sequential addition of a $Si(OH)_4$ monomer or by cyclisation reactions. They are schematically represented in order to show the connectivity between the SiO_4 monomers. Each SiO_4 is represented by a coloured dot in function of Q^n where n is the number of bridging oxygen atoms per SiO_4. The yellow zone indicates the growing steps that were fully investigated by DFT calculations including the activation barriers. A complete list of the equilibrium reactions is included in Table S2.

monomeric species, knowing that a basic pH is required to favour the oligomerisation reactions [35, 36].

Figure 1 shows the results of a first set of kMC calculations considering a reduced number of reactions (yellow background colour in Scheme 2) using Gibbs free energies issued directly from our DFT calculations. In the absence of a template, kMC simulations show that linear trimers and branched pentamers are the predominant species in solution. The absence of branched tetramers - although they are predicted as feasible by our DFT calculations - highlight that a direct examination of the free energy profiles is not sufficient to predict the outcome of such a large reaction network. It is striking that the branched tetramers form exclusively in the presence of organic templates, with steady state concentrations that are inversely proportional to the template's size (TMA^+>TEA^+>TPA^+). Also, we observe an inversion of the concentrations of the three major oligomers between TMA^+ (branched tetramer>linear trimer>branched pentamer) and TPA^+ (branched pentamer>linear trimer>branched tetramer). Notably, cyclic species are always in minor concentrations with respect to that of the others with the formation of four and five rings being slightly favoured by TEA^+. Finally, three rings are not observed in significant quantity in our simulations in line with previous theoretical works showing their higher reactivity in solution [18,37,38].

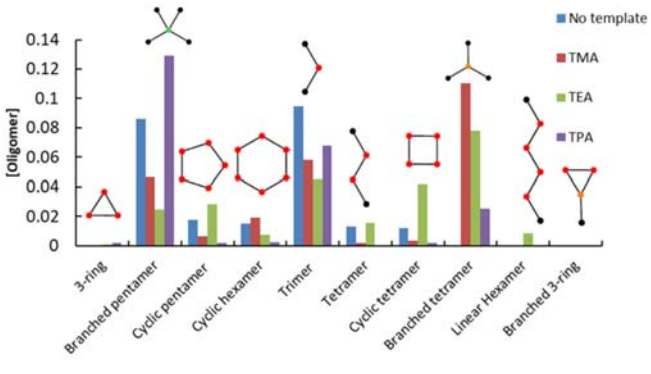

Figure 1. Steady state concentration of oligomers as obtained from kMC calculations using the reduced set of DFT-derived energy barriers of silica oligomers (yellow background in Scheme 2) and initial conditions of 1 $mol.L^{-1}$ of silica monomers at pH=9 and 350 K.

In order to understand the influence of the organic templates on the formation of more complex oligomers, we performed further kMC simulations using the extended reaction network illustrated in Scheme 2, *i.e.* up to octamers including linear and branched chains and cyclic oligomers up to an 8-membered ring. Doing so, we may be able to reach direct precursors of larger building blocks such as precursors of the double-four rings (D4R) found as main topological motives in many zeolite frameworks.

Exploring this extended reaction network with kMC simulations requires as many as 258 equilibrium reactions (including the formation of the different intermediate and transition state species), which would require the computation of more than 2000 activation barriers when taking into account the various templates (TMA^+, TEA^+ and TPA^+), which is obviously unrealistic. Thus, we have extended our database of activation barriers by means of the Brønsted-Evans-Polanyi (BEP) linear relationship (eq. 1) in order to predict those for longer oligomers [39].

$$\Delta G_{act}^{\neq} = \alpha \Delta G_r + \Delta G_0^{\neq} \qquad \text{eq. 1}$$

where $\Delta G_{act}^{\neq}$ is the activation barrier and ΔG_r is the free energy of reaction. The BEP model is an efficient way to calculate activation barriers for reactions of the same family of species [39] once the Gibbs free energies of reaction are estimated.

We have considered various BEP models both with and without organic template for the set of linear/branched/cyclic oligomers as obtained from DFT calculations. For all species, the activation energy of the first step, *i.e*. the formation of a new Si-O bond, correlates well with the corresponding reaction energy. The template does not affect this linear correlation as shown in Figure S3.a. The second step, *i.e.* the elimination of water, is, however, sensitive to the nature of the oligomer topology. While a linear correlation is found for branched and linear oligomers, it cannot be applied to the cyclisation of large cycles (Figure S3.b). This can be traced back to the fact that the mechanism for the release of water is strongly dependent on the oligomer conformation and size according to the NCI analysis. A great variability in the nature of intramolecular H-bonds involved is observed (see Figure S5). For this reason, BEP could not be applied to predict activation barriers for cyclic species greater than hexameric ones. For this reason, 7-membered and 8-membered rings were thus not included in the extended reaction network. This is, however, not a strong limitation considering the formation of long linear oligomers is rather unlikely based on our DFT calculations. Next, each type of reaction such as elongation (Q^1 to Q^2) or branching (Q^2 to Q^3 or Q^3 to Q^4) or small cycle formation is assumed having constant reaction energy regardless of the oligomer size. The corresponding activation energy is the one extrapolated using the BEP relationships, resulting in an extended database (see Table S2).

We can now treat by kMC simulations the complete set of reactions up to octamers (without 7-membered and 8-membered rings), a selection of which is shown in Scheme 2 (complete set in Table S2), using the reaction barriers calculated by DFT (yellow background) and those inferred from the BEP relationships as discussed above. A similar analysis in terms of steady state concentration of species that shown in Figure 1 is rendered extremely difficult due to the very large number of chemical species involved. It is noteworthy that running kMC simulations using the extended reaction scheme profoundly modifies the relative concentrations of species as reported in Figure 1, due to the full consumption of a number of small oligomers (*i.e*. trimers, tetramers…) for the purpose of growing larger ones (see Figure S6 representing species above 10% of the total concentration of species). To facilitate the comparison of our results (*i.e*. steady state concentrations of all species) with reported ^{29}Si NMR experiments on silica oligomerisation, we rather propose a quantitative analysis of the various oligomers concentrations in terms of the resulting Si-O-Si connectivity of all species taken together expressed as Q^n as defined earlier and illustrated in Scheme 2.

Our calculated Q^n at steady state are paralleled with the experimental ones collected from NMR in presence of $TMAda^+$ at different reaction times (N,N,N,-trimethyl-adamantammonium) (Figure 2.a) [28] or of TPA^+ over different initial precursor concentrations (Figure 2.b).[29] We consider that $TMAda^+$ is chemically close enough to TMA^+ to allow such a comparison. Our kMC calculations are in fairly good agreement with the relative experimental "bell curve" quantities for Q^1, Q^2, and Q^3 for reaction times shorter than 1h. Note that Q^4 is generally considered as the signature of nanoparticles formation, which are experimentally not detected before 1h reaction time [28] although our simulations suggest that Q^4 might be present in small proportion as highly branched oligomers. As for TPA^+ (Figure 2.b), our results also reflect the experimental tendency whereby the proportion of highly connected species (Q^2, Q^3, Q^4) decreases in favour of Q^1 when compared to TMA^+ (Figure 3.a). We would like to mention that Q^0 (a reactive species) is completely consumed due to the very favourable energy barriers of the condensation steps involving Q^0 and due to relatively small system size used in our kMC simulations. In addition, our simulations are restricted to only the anionic mechanism and the growth is limited to the sequential addition of monomers neglecting all other alternatives (dimer-dimer coupling …)[31].

In practice, the above analysis based on Figure 2 allows us to highlight the predominant chemical species identified as Q^1, Q^2, Q^3 and Q^4 represented in Figure 3. In the absence of template, there is no clear predominant species, with the branched heptamer representing up to ~11% (and other pentamer species with different concentrations, see Figure S6 for details). The addition of a template systematically sharpens the distribution of species, with one species dominating the solution mixture. On the one hand, TPA^+ still favours the formation of the same branched heptamer (up to 22.5%), in line with its ability to favour branching as already perceived in the first set of kMC simulations during the first steps of oligomerisation (Figure 1). On the other hand, TMA^+ and TEA^+ trigger the formation of branched 4-rings (up to 37.7% and 33.9%, respectively in Figure S6), which may be likely precursors of larger key building blocks such as the double 4-ring (D4R). D4R represents a common composite building unit (CBU) of about 39 known zeolite framework topologies, including synthetized structures (such as LTA, ACO and UFI)[40], as well as a large number of hypothetical structures [41, 42, 43].

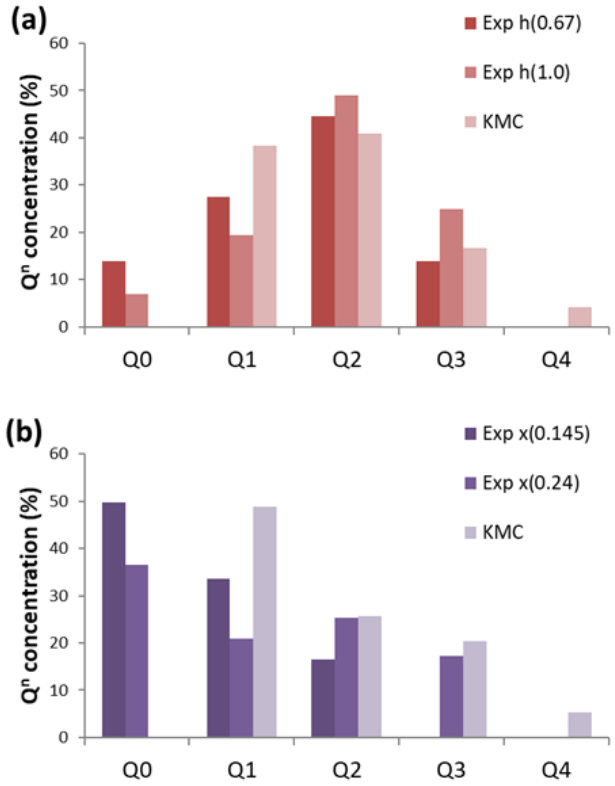

Figure 2. Comparison between kMC results using the extended set of reactions illustrated in Scheme 2 and ^{29}Si NMR experimental data with templates TMA^+ [28] (a) or TPA^+ [29](b) for the different silica oligomers in terms of their Si-O-Si connectivity expressed as Q^n where n is the number of bridging oxygen atoms per SiO_4. In (a), experimental results are reported after 0.67h and 1h of reaction while in (b), experimental results are reported at two initial reactant/template/water proportions (with x[Tetraethyl orthosilicate]/0.25[TPAOH]/20[H_2O] and x=0.145 and x=0.24).

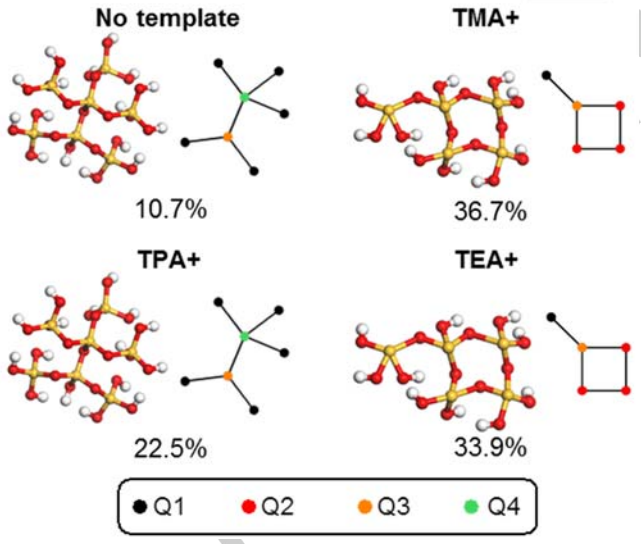

Figure 3. Predominant chemical species calculated in kMC calculations identified as Q^1, Q^2, Q^3 and Q^4.

Conclusion

We explored the oligomerisation process of silica in the presence of various organic templates (TMA^+, TPA^+ and TEA^+) using a strategy combining first principle DFT and kMC calculations. One key achievement is that we now propose an extended reaction path mechanism including as much as 258 equilibrium reactions and 242 different chemical species (including intermediates) up to octameric silica oligomers. In order to handle such a large reaction scheme for simulating the oligomerisation process, the energy barriers required in kMC calculations were inferred through the analysis of Brønsted-Evans-Polanyi (BEP) linear relationships from a restricted set of DFT-calculated energy barriers (monomer to pentamer), allowing the targeted extension up to octamers. The key advantage of such approach is the rapid access to barriers of these larger oligomers that would be unrealistic to compute using quantum methods.

The outcome of our kMC simulations, *i.e.* the steady state concentrations of oligomeric species, were directly compared with the experimentally available concentrations of Q^0, Q^1, Q^2, Q^3 and Q^4 species as collected from ^{29}Si NMR studies. Our multiscale computational approach is shown to consistently capture the impact of the organic template on the nature of the predominant species in solution. Importantly, our computational findings predict similar trends than those reported by the experimental findings. To the best of our knowledge, this direct comparison between kMC and experimental NMR on the early stages of oligomerisation has not been performed so far. With the combination of atomistic simulations with kMC, we have shown here that TPA^+ not only tends to favor Q^1 environment but more precisely branched oligomer (heptamer). On the other hand, TMA^+ and TEA^+ tend to favor Q^2 environment that can be related to a high concentration of branched 4-rings. We believe that our work provides a deeper understanding and control of the role played by organic templates in the early stages of the oligomerisation process. Future development may involve the identification of even more complex key structural units involved in the synthesis of zeolites and rationale strategies for the targeted synthesis of new topologies.

Conflict of interest

The authors declare no conflict of interest.

Keywords: kMC method • zeolite oligomerisation • DFT calculations • templates • Non Covalent Interactions

[1] Deniz Erdemir, Alfred Y. Lee, Allan S. Myerson, Acc. Chem. Res.**2009**, 42, 5, 621-629.
[2] Scott M. Woodley, Richard Catlow, Nat Mater. **2008** Dec; 7(12):937-46.
[3] Christine E. A. Kirschhock, Sebastien P. B. Kremer, Piet J. Grobet, Pierre A. Jacobs, Johan A. Martens, J. Phys. Chem. B, **2002**,106,19,4897-4900.
[4] Christopher T. G. Knight, Stephen D. Kinrade, J. Phys. Chem. B, **2002**, 106, 12, 3329-3332.
[5] Leen van Tendeloo, Mohamed Haouas, Johan A. Martens, C. E. A. Kirschhock, Eric Breynaert, Francis Taulelle, Faraday Discuss., **2015**,179, 437-449.
[6] Nicole Pienack, Wolfgang Bensch, Angew. Chem. Int. Ed. **2011**, 50, 2014 – 2034.

[7] Xue-Qing Zhang, Thuat T. Trinh, Rutger A. van Santen, Antonius P. J. Jansen, J Am Chem Soc. **2011** May 4;133(17):6613-25.
[8] Grant J. McIntosh, Phys.Chem.Chem.Phys., **2013**, 15, 3155.
[9] Grant J. McIntosh, Phys.Chem.Chem.Phys., **2013**, 15, 17496.
[10] Miguel J. Mora-Fonz, C. Richard A. Catlow, Dewi W. Lewis, Angew. Chem. Int. Ed. **2005**, 44, 3082 –3086.
[11] Miguel J. Mora-Fonz, C. Richard A. Catlow, Dewi W. Lewis, J. Phys. Chem. C **2007**,111,49,18155-18158.
[12] Thuat T. Trinh, Xavier Rozanska, Françoise Delbecq, Philippe Sautet, Phys. Chem. Chem. Phys., **2012**, 14, 3369-3380
[13] Ateeque Malani, Scott M. Auerbach, Peter A. Monson, J. Phys. Chem. C 2011, 115, 15988–16000.
[14] Miguel J. Mora-Fonz, C. Richard A. Catlow, Dewi W. Lewis, Phys Chem Chem Phys. **2008** Nov 21;10(43):6571-8.
[15] Xue-Qing Zhang, Thuat T. Trinh, Rutger A. van Santen, Antonius P. J. Jansen, J. Phys. Chem. C **2011**, 115, 9561–9567.
[16] Mahmoud Moqadam, Enrico Riccardi, Thuat T. Trinh, Anders Lervik, Titus S. van Erp, Phys. Chem. Chem. Phys., **2017**, 19, 13361-13371.
[17] Thuat T. Trinh, Khanh-Quang Tran, Xue-Qing Zhang, Rutger A. van Santenc, Evert Jan Meijer, Phys. Chem. Chem. Phys., **2015**,17, 21810-21818.
[18] J.Mora-Fonz, C.R.A.Catlow, D.W.Lewis, **2005**, Stud. Surf. Sci. 158, 295–302.
[19] Veronique Van Speybroeck, Karen Hemelsoet, Lennart Joos, Michel Waroquier, Robert G. Bell, C. Richard A. Catlow, Chem. Soc. Rev., **2015**, 44, 7044-7111.
[20] Chao-Shiang Yang, José Miguel Mora-Fonz, C. Richard A. Catlow, J. Phys. Chem. C **2011**, 115, 24102–24114.
[21] McIntosh GJ, Phys Chem Chem Phys. **2012** Jan 14;14(2):996-1013.
[22] McIntosh GJ, Phys Chem Chem Phys. **2013** Mar 7;15(9):3155-72.
[23] Grant J. McIntosh, Phys. Chem. Chem. Phys., **2013**,15, 17496-17509.
[24] Xue-Qing Zhang, Thuat T. Trinh, Rutger A. van Santen, Antonius P. J. Jansen, J. Phys. Chem. C **2012**, 116, 1, 1622-1623.
[25] Xue-Qing Zhang, Rutger A. van Santen, Antonius P. J. Jansen, Phys. Chem. Chem. Phys., **2012**, 14, 11969–11973.
[26] Thuat T. Trinh, Antonius P. J. Jansen, Evert Jan Meijer, Chemphyschem. **2009** Aug 3;10(11):1775-82.
[27] Gaussian 09, Revision A.02, M. J. Frisch, G. W. Trucks, H. B. Schlegel, G. E. Scuseria, M. A. Robb, J. R. Cheeseman, G. Scalmani, V. Barone, G. A. Petersson, H. Nakatsuji, X. Li, M. Caricato, A. Marenich, J. Bloino, B. G. Janesko, R. Gomperts, B. Mennucci, H. P. Hratchian, J. V. Ortiz, A. F. Izmaylov, J. L. Sonnenberg, D. Williams-Young, F. Ding, F. Lipparini, F. Egidi, J. Goings, B. Peng, A. Petrone, T. Henderson, D. Ranasinghe, V. G. Zakrzewski, J. Gao, N. Rega, G. Zheng, W. Liang, M. Hada, M. Ehara, K. Toyota, R. Fukuda, J. Hasegawa, M. Ishida, T. Nakajima, Y. Honda, O. Kitao, H. Nakai, T. Vreven, K. Throssell, J. A. Montgomery, Jr., J. E. Peralta, F. Ogliaro, M. Bearpark, J. J. Heyd, E. Brothers, K. N. Kudin, V. N. Staroverov, T. Keith, R. Kobayashi, J. Normand, K. Raghavachari, A. Rendell, J. C. Burant, S. S. Iyengar, J. Tomasi, M. Cossi, J. M. Millam, M. Klene, C. Adamo, R. Cammi, J. W. Ochterski, R. L. Martin, K. Morokuma, O. Farkas, J. B. Foresman, and D. J. Fox, Gaussian, Inc., Wallingford CT, 2016.
[28] Einar A. Eilertsen, Mohamed Haouas, Ana B. Pinar, Nathan D. Hould, Raul F. Lobo, Karl P. Lillerud, Francis Taulelle, Chem. Mater. **2012**, 24, 3, 571-578.
[29] Sanja Bosnar, Tatjana Antonić Jelić, Josip Bronić, Maja Dutour Sikirić,Suzana Šegota, Vida Čadež, Vilko Smrečki, Ana Palčić, Boris Subotić, J. Phys. Chem. C, **2018**, 122, 17, 9441-9454.
[30] Claire E. White, John L. Provis, Thomas Proffen, Jannie S. J. van Deventer, J. Phys. Chem. C **2011**, 115, 9879–9888.
[31] Marine Ciantar, Caroline Mellot-Draznieks, Carlos Nieto-Draghi, J. Phys. Chem. C **2015** 119, 52,28871-28884.
[32] Thuat T. Trinh, Antonius P. J. Jansen, Rutger A. van Santen, Evert Jan Meijer, Phys. Chem. Chem. Phys., **2009**, 11, 5092–5099.
[33] Julia Contreras-García, Erin R. Johnson, Shahar Keinan, Robin Chaudret, Jean-Philip Piquemal, David N. Beratan, Weitao Yang, J. Chem. Theory Comput. 2011, 7, 3, 625-632.
[34] Erin R. Johnson, Shahar Keinan, Paula Mori-Sánchez, Julia Contreras-García, Aron J. Cohen, Weitao Yang, J. Am. Chem. Soc. 2010, 132, 18, 6498-6506.
[35] White, C. E., & Provis, J. L, 2012, The Journal of Physical Chemistry C, 116(1), 1619–1621.
[36] Knight, C. T. G., & Kinrade, S. D, 2001, Studies in Plant Science, 8(C), 57–84.
[37] J. C. G. Pereira, C. R. A. Catlow, G. D. Price, J. Phys. Chem. A, **1999**, 103, 17, 3252-3267.
[38] J. C. G. Pereira,C. R. A. Catlow,G. D. Price, J. Phys. Chem. A, **1999**, 103, 17, 3268-3284.
[39] Hervé Toulhoat , Pascal Raybaud, J. Catal. **2003**, 216, 63–72.
[40] International zeolite association (IZA) database (https://europe.iza-structure.org/IZA-SC/search-results_fw.php, accessed on 07/10/2020)
[41] Jibo Hu, Xusen Guo, Jianwen Chen, Xuehua Liu, Junxiong Qu, Jinwei Wang, Junrui Yang, Jiuxing Jiang, Micropor. Mesopor. Mat., **2020**, 298, 110050.
[42] Xuehua Liu, Soledad Valero, Estefania Argente, German Sastre, Faraday Discuss., **2018**, 211, 103-115.
[43] Caroline Mellot-Draznieks, Stéphanie Girard, Gérard Férey. J. Am. Chem. Soc., **2002**, 124, 15326-1535.

Entry for the Table of Contents

Insert graphic for Table of Contents here.

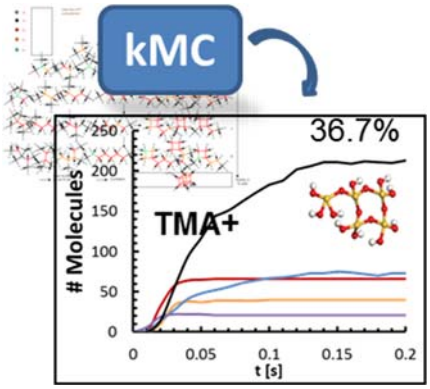

DFT and kMC calculations are combined to investigate the impact of the most commonly used organic template molecules (tetrapropylamine-TPA+, tetraethylamine-TEA+ and tetramethylamine-TMA+) both on the reaction energy profiles and the kinetics of formation of silica oligomers. The extended reaction path mechanism includes as much as 258 equilibrium reactions and 242 different chemical species up to octameric species. The templating agent is shown to produce higher concentration of 4-membered ring intermediates.

Institute and/or researcher Twitter usernames: ((optional))